Charge inversion by multivalent ions: Dependence on dielectric constant and surface-charge density

K. Besteman, M. A. G. Zevenbergen, and S. G. Lemay
Kavli Institute of Nanoscience, Delft University of Technology, 2628 CJ Delft, The Netherlands
(Received 8 July 2005; published 1 December 2005)

Charge inversion occurs when the effective charge of a surface exposed to solution reverses polarity due to an excess of counterions accumulating in the immediate vicinity of the surface. Using atomic force spectroscopy, we have directly measured the effect on charge inversion of changing the dielectric constant of the solvent and the surface-charge density. Both decreasing the dielectric constant and increasing the bare surface-charge density lower the charge-inversion concentration. These observations are consistent with the theoretical proposal that spatial correlations between ions are the dominant driving mechanism for charge inversion.

DOI: 10.1103/PhysRevE.72.061501 PACS number(s): 82.45.Gj, 82.45.Mp, 07.79.Lh

I. INTRODUCTION

Screening by mobile ions dominates electrostatic interactions in electrolytes, making it a very important element of polymer physics, nanofluidics, colloid science, and molecular biophysics. In the presence of multivalent ions, counterintuitive phenomena occur such as attraction between like-charged molecules [1] and its converse, repulsion between oppositely charged objects [2]. Similarly, the electrophoretic mobility of charged colloids can reverse sign in the presence of multivalent ions [3,4], a phenomenon known as *charge inversion* or *overcharging*. Charge inversion has also been observed and studied using numerical simulations [5,6].

Early observations of the charge inversion of oxides by metal ions were interpreted in terms of specific chemical binding between the multivalent ions and the surface being screened [3,7–9]. This mechanism necessarily relies on the detailed chemical structure of the substances involved, for example the propensity of metal ions to form hydroxides [3,7–9]. Theory, however, suggests that such specific interactions are not necessary for charge inversion to take place [10]. In particular, it has been argued that spatial correlations, ignored in conventional mean-field descriptions of screening on which much of our intuition is based, are highly relevant for multivalent ions and naturally lead to charge inversion. We indeed recently showed [2] that, for a variety of ions, charge inversion is an equilibrium effect that depends very strongly on the valence Z of the ions but can be largely insensitive to their chemical properties, in agreement with these theoretical predictions.

Here we extend these measurements by exploring the dependence of charge inversion on the dielectric constant of the medium ϵ and the bare surface-charge density σ_{bare}. We compare the results with the predictions from both specific binding and ion-correlation theories.

II. THEORETICAL BACKGROUND

Charge inversion occurs when the concentration of multivalent ions in the bulk solution, c, exceeds the so-called charge-inversion concentration c_0. We are particularly interested in probing c_0 for two related reasons. First, c_0 can be determined experimentally without recourse to any particular model. Second, it is a quantity that is particularly amenable to theoretical treatment: since the surface is neutralized at $c=c_0$, fewer assumptions are necessary regarding the structure of the double layer. In this section we first summarize the derivation of a simple, mean-field expression for c_0 in terms of specific binding of multivalent ions to the surface, then indicate how this expression is modified by spatial correlations between multivalent ions at the surface.

Consider a surface with bare charge density σ_{bare} in equilibrium with an electrolyte. For large σ_{bare} the double layer is conventionally divided into two regions: the diffuse layer, in which the Poisson-Boltzmann (PB) equation holds, and, close to the surface, the so-called Stern layer. In our simple model, the latter contains a two-dimensional layer of ions (predominantly multivalent in our case) located a distance d_s away from the surface containing a charge density σ_{Stern}. The parameter d_s represents the finite size of the ions. For simplicity the charge density is commonly taken to be zero in the range $0<x<d_s$, where x is the distance from the surface. It is further assumed that multivalent ions are held in the Stern layer not only by electrostatic interaction with the charged surface, but also by a chemical interaction. Specifically, it is assumed that local interactions between each ion and the surface and/or the solvent contribute a change in free energy $\Delta\mu^{0*}$ upon taking one multivalent from the bulk to the Stern layer. The parameter $\Delta\mu^{0*}$ includes any complex formation between the ion and the surface. It can in general be expected to depend on specific properties of the system such as chemical composition, surface structure, and lipophilicity of both the ions and the surface. $\Delta\mu^{0*}$ cannot be predicted reliably at this time: in comparing to data it is typically treated as an empirical fitting parameter.

In equilibrium, the electrochemical potential of the multivalent ions in the bulk is equal to that of multivalent ions in the Stern layer [11]. These electrochemical potentials are, respectively, $\mu_b=\mu_b^0+kT\ln(c/c_{\max})+Ze\psi(\infty)$ and $\mu_s=\mu_s^0+kT\ln(c_s/c_{s,\max})+Ze\psi(d_s)$. Here the activity coefficients have been set to unity [11], μ_s^0 and μ_b^0 are constant parameters such that $\mu_s^0-\mu_b^0=\Delta\mu^{0*}$, c and $c_{\max}$ are, respectively, the concentration and maximum concentration of multivalent ions in the bulk, c_s and $c_{s,\max}$ are, respectively, the two-

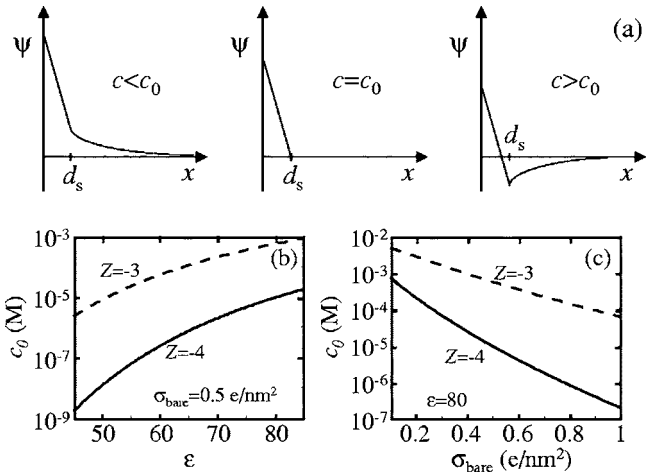

FIG. 1. (a) Sketch of the electrostatic potential ψ as a function of the distance x from a surface with constant σ_{bare} for the cases $c<c_0$ (no charge inversion), $c=c_0$ (neutralization of the surface), and $c>c_0$ (charge inversion). (b) Dependence of the charge-inversion concentration c_0 on ϵ as predicted by spatial correlation theory, Eq. (3), with $\Delta\mu^0=0$, $r=0.5$ nm, and $\sigma_{\text{bare}}=0.5\ e/\text{nm}^2$. (c) Same as (b) for dependence on bare surface-charge density σ_{bare} with $\epsilon=80$.

dimensional concentration and maximum two-dimensional concentration of multivalent ions in the Stern layer, and $\psi(x)$ is the electrostatic potential as a function of the distance x from the surface. k, T, and $-e$ are the Boltzmann constant, the absolute temperature, and the electron charge, respectively. Equilibrium thus requires that

$$kT\ln\left(\frac{c_s}{c_{s,\max}}\right)+\Delta\mu^{0*}+Ze\psi(d_s)=kT\ln\left(\frac{c}{c_{\max}}\right), \qquad (1)$$

where the potential in the bulk $\psi(\infty)$ was taken as zero.

In the region $0<x<d_s$ the potential ψ varies linearly with x to the value $\psi(d_s)$. For $x>d_s$, $\psi(x)$ drops to the bulk value according to the PB equation. Figure 1(a) sketches the potential $\psi(x)$ for the cases when the Stern layer almost compensates the surface charge ($c<c_0$, $|\sigma_{\text{Stern}}|<|\sigma_{\text{bare}}|$), fully compensates the surface charge ($c=c_0$, $|\sigma_{\text{Stern}}|=|\sigma_{\text{bare}}|$, $\psi(d_s)=0$), and overcompensates the surface charge ($c>c_0$, $|\sigma_{\text{Stern}}|>|\sigma_{\text{bare}}|$).

At $c=c_0$ the bare surface charge is entirely compensated by the charge in the Stern layer, thus $c_s=|\sigma_{\text{bare}}/Ze|$ and $\psi(d_s)=0$. Further taking on geometrical grounds that $c_{s,\max}/c_{\max}=2r$, where r is the radius of an ion, Eq. (1) then yields for the charge-inversion concentration

$$c_0=\left|\frac{\sigma_{\text{bare}}}{2rZe}\right|\exp\left(\frac{\Delta\mu^{0*}}{kT}\right). \qquad (2)$$

For specific binding to account for charge inversion, $\Delta\mu^{0*}$ must be negative and several times kT in magnitude.

Real surfaces become charged in an electrolyte by the dissociation of charged groups (ions) from the surface or association of charged groups to the surface [12]. Such chemical equilibrium between surface sites and charge-determining ions renders σ_{bare} dependent on the concentration of charge-determining ions at the surface, and thus on the bulk concentration of all ions in the solution including the multivalent ions. This so-called charge regulation does not affect the condition for charge inversion given by Eq. (2), however, and only enters Eq. (2) implicitly via σ_{bare}. In situations where charge regulation plays a significant role, the value of σ_{bare} must be obtained self-consistently for the condition $\psi(d_s)=0$ and $c=c_0$. Since experimentally $\sigma_{\text{bare}}(c_0)$ is difficult to determine independently, we will treat it as an unknown parameter.

So far we have discussed the influence of regulation of the bare surface charge due to equilibrium with a bulk reservoir. Additional regulation effects can occur when two surfaces are brought into such proximity to each other that they influence each other's double layers. This effect can even result in a reversal of the force of interaction as a function of the distance between the surfaces [13–15]. Since our experiments mostly focus on long-range interactions (distance greater than 2λ, where λ is the Debye length) and that such regulation effects become important at shorter range, we do not consider these effects further here.

Several authors have attempted descriptions beyond the mean-field one outlined above and incorporated the role of spatial correlations between multivalent ions in the Stern layer. Here we concentrate on the formalism introduced by Shklovskii [16], which hinges on the theoretical observation that multivalent ions must form a strongly correlated ionic liquid in the Stern layer of surfaces with high σ_{bare}. This formalism leads to simple analytical expressions for the charge-inversion concentration c_0. The development parallels that given above, with the additional refinement that $\Delta\mu^{0*}$ is replaced by $\Delta\mu^0+\mu_c$. Here $\Delta\mu^0$ represents hydration and specific binding effects while μ_c accounts for spatial interactions between multivalent ions in the Stern layer. The predicted value for the charge-inversion concentration is then

$$c_0=\left|\frac{\sigma_{\text{bare}}}{2rZe}\right|\exp\left(\frac{\mu_c}{kT}\right)\exp\left(\frac{\Delta\mu^0}{kT}\right) \qquad (3)$$

with μ_c given by [16,17]

$$\mu_c=-kT(1.65\Gamma-2.61\Gamma^{1/4}+0.26\ln\Gamma+1.95) \qquad (4)$$

and the interaction parameter Γ by

$$\Gamma=\frac{1}{4kT\epsilon\epsilon_0}\sqrt{\left|\frac{e^3Z^3\sigma_{\text{bare}}}{\pi}\right|}, \qquad (5)$$

where ϵ_0 is the permittivity of free space. This theory holds for $\Gamma\gg 1$ [16,18], which is typically fulfilled for $Z\geqslant 3$. For example, when $Z=3$, $\sigma_{\text{bare}}=0.5\ e/\text{nm}^2$, and $\epsilon=80$, the value of Γ is 4.6. Calculated values of Γ from our experiments are in the range $3\lesssim\Gamma\lesssim 8$. For $\Gamma\gg 1$, μ_c is approximately equal to the first term in Eq. (4), yielding $\mu_c\propto-\sqrt{|\sigma_{\text{bare}}Z^3|}/\epsilon$. Thus while we use the full expression for μ_c in our calculations, the approximation is expected to correctly predict the qualitative trends. For monovalent salt ($Z=1$) at room temperature, $\Gamma\lesssim 1$ and correlation effects do not play a significant role [16,18,19].

Equation (3) predicts that charge inversion can occur even in the absence of specific adsorption ($\Delta\mu^0=0$). Correlations are then solely responsible for charge inversion. The depen-

dence of c_0 on Z, ϵ, and σ_{bare} from Eqs. (3)–(5) is plotted in Fig. 1.

III. EXPERIMENTAL METHODS

We have determined the charge-inversion concentration through a direct measurement of the electrostatic interaction between two oppositely charged surfaces, as described previously [2]. In short, we used a Digital Instrument NanoScope IV Atomic Force Microscope (AFM) to measure the force F between the surfaces versus their separation d in different concentrations c of an asymmetric Z:1 electrolyte. The sign of the force far from contact unambiguously yields the effective polarity of the surface being screened by the multivalent counterion.

The negatively charged surface consisted of a silica bead glued to an AFM cantilever. The AFM cantilever was heated with a soldering iron. Using a micromanipulator, a small amount of epoxy resin (EPI-REZ 3522-W-60) was deposited on the hot tip of the cantilever. Next, a 10 μm silica sphere (G. Kisker Gbr) was deposited from a glass microscope slide on the tip of the cantilever. Upon cooling, the resin solidified and the bead remained attached to the end of the tip [20]. In contact with water silica gets charged by the dissociation of silanol groups, $(\text{Si})\text{OH} \rightleftarrows (\text{Si})\text{O}^- + \text{H}^+$, where (Si) is a silicon atom at the surface.

The positively charged amine-terminated surface was prepared from a silicon dioxide surface. A silicon substrate with 300–500 nm thermally grown oxide was first immersed in a 3:1 mixture of sulfuric acid and hydrogen peroxide for 15 min and rinsed with deionized Milli-Q filtered water (mq water). In a glove box containing a nitrogen environment, it was then immersed in a 0.1% solution of 1-trichlorosilyl-11-cyanoundecane $[\text{NC}(\text{CH}_2)_{11}\text{SiCl}_3]$ (Gelest) in toluene for 30 min and rinsed in clean toluene. The trichlorosilane group of the molecule binds covalently to the surface. The substrate was then sonicated in toluene, chloroform, and again toluene, each for 5 min in an acid hood. Back in the glove box, it was immersed in a 20% solution of Red Al (Sigma-Aldrich) in toluene for 5 h and afterwards rinsed in clean toluene. The Red Al reduces the cyano group to an amino group. Finally the substrate was sonicated in, respectively, toluene, acetone, mq water, nitric acid (pH 2), and mq water each for 5 min and blown dry. The substrate was kept under nitrogen atmosphere until used. In contact with water the amino group can take up a proton, $(\text{Si})-\text{R}-\text{NH}_2 + \text{H}^+ \rightleftarrows (\text{Si})-\text{R}-\text{NH}_3^+$.

The AFM cantilever (ThermoMicroscope Microlever) had a nominal force constant of about 0.03 N/m, as specified by the manufacturer. Absolute values of force shown here are based on this value.

We present results using five different multivalent ions. The same molecule in two different charge states, iron(II) hexacyanide $[\text{Fe}(\text{CN})_6]^{4-}$ (r=443 pm) and iron(III) hexacyanide $[\text{Fe}(\text{CN})_6]^{3-}$ (r=437 pm) [21–23], both with K^+ counterions, was used to investigate charge inversion on the positively charged amine-terminated surface. Three positive trivalent ions with a different chemical composition were used to investigate charge inversion on the negatively charged silica bead. All three have Cl^- counterions. Lanthanum La^{3+} is a metal ion with a first hydration shell consisting of 8–9 water molecules (radius r of the complex 398 pm [21–24]). Ruthenium(III) hexamine $[\text{Ru}(\text{NH}_3)_6]^{3+}$ contains a Ru(III) core surrounded by six NH_3 groups (r=364 pm [21–23]). Cobalt(III) sepulchrate $[\text{CoC}_{12}\text{H}_{30}\text{N}_8]^{3+}$ is a caged cobalt complex with CH_2 groups exposed to the solvent (r =445 pm [25]), and is expected to be less hydrophillic than the other two.

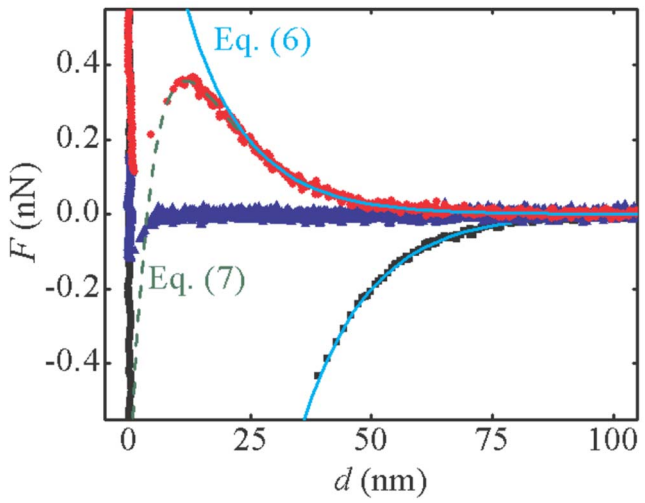

FIG. 2. (Color online) Measurements of the force F versus separation d in a pH 6 solution with 0.5 mM KCl (squares, bottom curve), after adding 50 μM $[\text{Fe}(\text{CN})_6]^{4-}$ to the 0.5 mM KCl solution (circles, top curve), and in a 1 M KCl solution (triangles, middle curve). The three measurements used the same amine-terminated surface and silica bead. Fits to Eq. (6) are shown as solid lines. A fit to Eq. (7) is shown as a dashed line.

For each series of measurements, $F(d)$ was first measured in a monovalent electrolyte. Consecutive measurements with increasing concentrations of multivalent ions in addition to the monovalent salt were then carried out. Each new solution was pumped through the AFM liquid cell (volume $\approx$50 μL) at a rate of 0.15 ml/min for 5–15 min before obtaining $F(d)$ curves, thus allowing the surface to equilibrate with the solution and insuring that c was not diminished by ions screening the surface. At the end of each experiment, the lowest concentration of multivalent ions was pumped back into the fluid cell and $F(d)$ curves were once again obtained.

IV. FORCE-DISTANCE CURVES

Figure 2 shows the measured force F versus the distance d between a silica bead and an amine-terminated surface. Three curves are shown that correspond to three different electrolytes. The observed $F(d)$ curves are dramatically different for the three cases.

The curve represented by squares (bottom curve) was obtained in a solution containing 0.5 mM monovalent salt. At bead-surface separations less than about 75 nm, an attractive (negative) force was observed that increased in magnitude with decreasing separation. Below about 35 nm separation, the attractive force gradient exceeded the spring constant of

the cantilever and the bead snapped to the surface.

The curve represented by circles (top curve) was obtained in a solution containing 50 μM $-4:+1$ salt in addition to the monovalent salt. A repulsive (positive) force was clearly observed below about 55 nm separation, which we interpret as indicating that charge inversion of the positive surface has occurred. The force increased with decreasing distance until $d=13$ nm. For d in the range 8–13 nm, the force instead decreased with decreasing distance. Below 8 nm snap-in occurred.

The curve represented by triangles (middle curve) was obtained in a solution containing 1 M monovalent salt. The Debye screening length λ of this solution is ≈ 0.3 nm, and hence electrostatic interactions are expected to play no role except at extremely small separations. The observed force remained zero until the distance d was only about 5 nm. Below this distance a weak attractive force was observed which we attribute to van der Waals forces. The data show that van der Waals forces are negligible for $d>10$ nm.

In order to quantitatively describe the $F(d)$ curves, we distinguish between two main regimes depending on whether the separation d is greater or smaller than about twice the Debye length λ of the solution.

In the regime $d \gtrsim 2\lambda$, the force F between the silica bead and amine-terminated surface is expected from the Poisson-Boltzmann equation to decay exponentially with d:

$$F(d) = F_0 \exp(-d/\lambda), \quad d \gtrsim 2\lambda. \tag{6}$$

The parameter F_0 is not the real force at zero separation, but rather the value of the force when the functional form valid far from the surface is extrapolated to the surface. Theoretically $F_0 \propto \sigma_b^\star \sigma_s^\star$, where $\sigma_b^\star$ and $\sigma_s^\star$ are the so-called renormalized surface-charge densities of the silica bead and of the amine-terminated surface, respectively. $\sigma_b^\star$ and $\sigma_s^\star$ are related to the net surface-charge densities of the bead and the amine-terminated surface, σ_b and σ_s, which include both the bare surface charge and the charge in the Stern layer. At low net surface-charge density $|\sigma_{b,s}| < \sigma_{\max} \approx 4kT\epsilon\epsilon_0/e\lambda$, the renormalized charge densities are simply equal to the net charge densities: $\sigma_{b,s}^\star = \sigma_{b,s}$. At higher net charge densities, $\sigma_{b,s}^\star$ saturates at $\sigma_{\max}$.

Because we use oppositely charged surfaces and asymmetric $Z:1$ electrolytes and correlation effects are only relevant for $Z>1$, charge inversion is only expected to occur at one of the surfaces. The other surface, screened predominantly by monovalent ions, can thus be thought of as a constant probe. Near charge inversion, F_0 is thus approximately proportional to the net surface-charge density of the surface being screened by multivalent ions, σ_b or σ_s, and the sign of the force unambiguously yields the polarity of this net surface charge. Note that, strictly speaking, the value of $\sigma^\star \approx \sigma_{\max}$ for the probe is not constant since it depends linearly on λ^{-1} and more subtly on the valence of the ions [26]. This introduces a small systematic error in the fitted value of c_0, but does not affect the measured *sign* of the force.

The solid lines in Fig. 2 show fits of the data to Eq. (6) in which F_0 and λ are used as fitting parameters. The fitted values of λ are 13.9 and 12.6 nm for the measurements in the monovalent electrolyte and in the electrolyte containing multivalent ions, respectively. The calculated values of λ for these electrolytes are 13.6 and 9.6 nm, respectively. Equation (6) gives less good quantitative agreement with the data obtained in the charge-inversion regime. It also fails to capture the decrease in F with decreasing d at short range in this case. This is not unreasonable since Eq. (6) becomes increasingly inaccurate with decreasing d. The leading correction [14] yields

$$F = F_0 \exp(-d/\lambda) + F_1 \exp(-2d/\lambda), \tag{7}$$

which reduces to Eq. (6) at large enough separations. Here $|F_1| \propto (\sigma_b^{\star 2} + \sigma_s^{\star 2})$. Near charge inversion of one of the two surfaces, the F_1 term in Eq. (7) becomes much more prevalent. This is because $\sigma^\star$ vanishes at c_0 for the surface being charge inverted while $\sigma^\star$ of the other surface remains $\approx \sigma_{\max}$, leading to a vanishing F_0 and a largely unaffected F_1. Equation (6) can therefore be expected to be less accurate near charge inversion, as observed.

The sign of F_1 depends on the boundary conditions of the system: surfaces with constant net surface-charge density give positive values of F_1 (repulsive force), while surfaces at constant potential give negative values of F_1 (attractive force) [13–15,20]. A surface whose net surface charge is strongly regulated behaves as being at constant potential, and this is also the case that is predicted to apply for the net surface charge in the presence of a strongly correlated Stern layer [14].

The dashed line in Fig. 2 gives a fit of Eq. (7) to the measurement in the presence of multivalent ions, where F_0, F_1, and λ are used as fitting parameters. The fitted value of F_1 is negative, implying that the surface screened by multivalent ions indeed behaves as if held at a constant potential. The fitted value of λ is 11.6 nm, in better agreement with the expected value than the fit to Eq. (6).

In the remainder of this paper we concentrate on the regime where both $d>2\lambda$ and van der Waals forces are small ($d>10$ nm), where we can reliably fit to Eq. (6). Under these conditions and near charge inversion, F_0 is approximately proportional to the net surface-charge density of the surface being screened by multivalent ions and the sign of the force unambiguously yields the polarity of this net surface charge.

V. DIELECTRIC CONSTANT ϵ

We have measured the influence of the dielectric constant of the solvent on the charge-inversion concentration by using water-alcohol mixtures as the solvent. These were prepared by mixing solutions of 2 mM KOH and 2 mM HCl (both in water) to the desired *p*H value, then diluting with mq water and/or ethanol to obtain mixtures with dielectric constant $\epsilon = 80$ (only water), 68 (75% water, 25% ethanol) and 54 (50% water, 50% ethanol). The values of the dielectric constant were obtained by interpolating between tabulated values for water-ethanol mixtures [27].

Figure 3 shows an experiment where the same amine-terminated surface was charge inverted with $[Fe(CN)_6]^{4-}$ in electrolytes with different dielectric constants. The same silica bead was used during the entire experiment. After changing the dielectric constant of the solution, a part of the

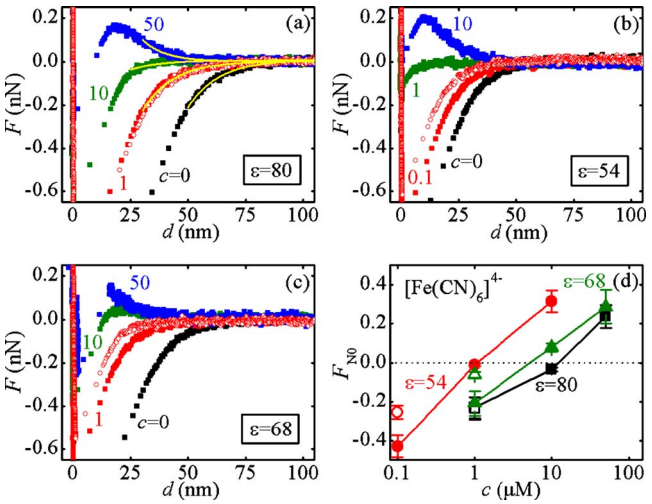

FIG. 3. (Color online) Measurement of the force F versus separation d in solvents with different dielectric constants: $\epsilon=80$ (a), $\epsilon=54$ (b), and $\epsilon=68$ (c). The electrolyte contained $[Fe(CN)_6]^{4-}$ and 0.5 mM KCl at pH 6.0±0.5. The numbers next to each curve indicate the multivalent ion concentration c in μM. All measurements were performed with the same amine-terminated surface and silica bead. In (a), fits to Eq. (6) are shown as lines. (d) Normalized force F_{N0} versus c for $\epsilon=80$ (squares), $\epsilon=54$ (circles), and $\epsilon=68$ (triangles). In each panel the open symbols represent the last measurement performed to check the reversibility of the charge inversion.

amine-terminated surface that had not been in contact with the electrolyte during the previous measurement was used. The data clearly show that a lower concentration of multivalent ions is required to cause charge inversion when the dielectric constant is reduced.

We fitted $F(d)$ curves to Eq. (6) in the range $d>2\lambda$ and extracted the force F_0. Because it is difficult to accurately fit λ when the force is very small, the value of λ was only fitted for the curve with $c=0$ and corrected using the standard expression when $c>0$. Figure 3(a) shows such fits to Eq. (6) as lines through the data.

Figure 3(d) shows F_0 versus multivalent ion concentration c. Each point represents the average of five separate fits. To facilitate comparison between different curves, the value of F_0 was normalized to its value when $c=0$ for each curve: $F_{N0}(c)=F_0(c)/F_0(0)$. We estimate the charge-inversion concentration c_0 by linearly interpolating between the data points immediately above and below $F_{N0}=0$ on the lin-log scale. The resulting values of c_0 are 12, 5, and 1 μM for $\epsilon=80$, 68, and 54, respectively. Thus lowering the dielectric constant from 80 to 54 causes a decrease of the charge-inversion concentration by a factor ≈ 10.

At the end of each experiment, $F(d)$ was measured at the same concentration c of multivalent ions as was used at the beginning of the experiment (open circles in Fig. 3). In water, the resulting curve was usually identical to that measured at the beginning of the experiment [see, for example, Fig. 3(a)]. In water-ethanol mixtures, however, the magnitude of the force often decreased after prolonged exposure [Figs. 3(b) and 3(c)]. This was also observed in the absence of multivalent ions, indicating that exposure to ethanol induced a slow decrease of the magnitude of the surface charge. To

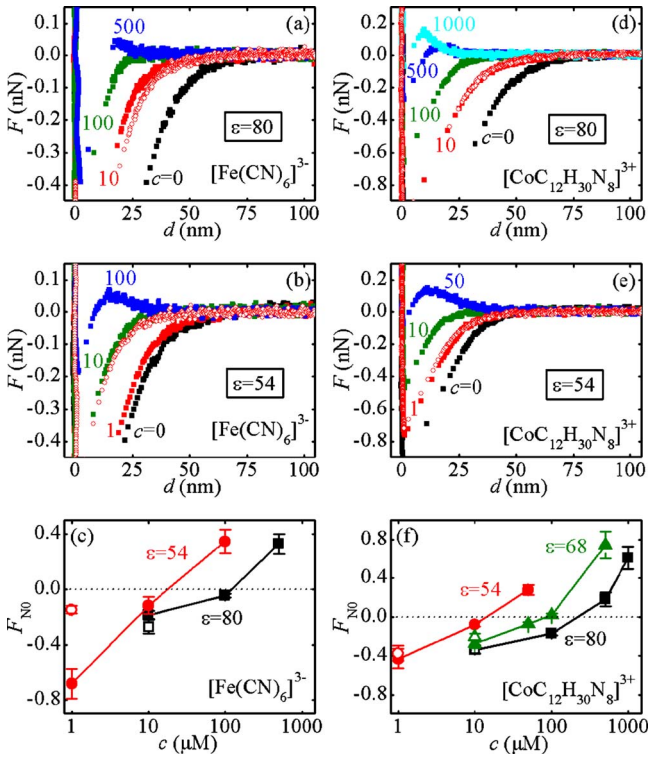

FIG. 4. (Color online) Force F versus separation d in the presence of $[Fe(CN)_6]^{3-}$ (a),(b) or $[CoC_{12}H_{30}N_8]^{3+}$ (d),(e) with solvents having dielectric constants $\epsilon=80$ (a),(d) or $\epsilon=54$ (b),(e). The electrolyte contained 0.5 mM ($\epsilon=80$) or 0.25 mM ($\epsilon=54$) KCl with pH 6.0±0.5 for the $[Fe(CN)_6]^{3-}$ measurements and 0.5 mM KCl with pH 7.0±0.5 for the $[CoC_{12}H_{30}N_8]^{3+}$ measurements. (c),(f) F_{N0} versus c using $[Fe(CN)_6]^{3-}$ (c) and $[CoC_{12}H_{30}N_8]^{3+}$ (f) for $\epsilon=80$ (squares), $\epsilon=54$ (circles) and $\epsilon=68$ (triangles). The values of c_0 for $[Fe(CN)_6]^{3-}$ are 120 and 18 μM for $\epsilon=80$ and 54, respectively. The values of c_0 for $[CoC_{12}H_{30}N_8]^{3+}$ are 220, 88, and 14 μM for $\epsilon=80$, 68, and 54, respectively.

minimize the influence of this on further analysis, we compare data that were obtained on surfaces exposed to solution for approximately the same duration.

Figure 4 shows similar experiments using the multivalent ions $[Fe(CN)_6]^{3-}$ and $[CoC_{12}H_{30}N_8]^{3+}$, and 0.5mM KCl as monovalent salt. When decreasing ϵ from 80 to 54, c_0 decreased by a factor 7 for $[Fe(CN)_6]^{3-}$ and 16 for $[CoC_{12}H_{30}N_8]^{3+}$.

Figure 5 shows a comparison between the three trivalent positive ions. In each case decreasing ϵ causes a decrease in c_0 irrespective of chemical structure. The values of c_0 for the three ions are within a factor of 2 at $\epsilon=80$ and within a factor of 4 at $\epsilon=54$. The decrease in c_0 when decreasing ϵ from 80 to 54 is a factor of 23 for $[Ru(NH_3)_6]^{3+}$, 47 for La^{3+}, and 30 for $[CoC_{12}H_{30}N_8]^{3+}$ for these particular surfaces. In these measurements HEPES (4-(2-hydroxyethyl)piperazine-1-ethanesulfonic acid) buffer was used as the monovalent salt because of the atypical behavior of La^{3+}, namely, the pH of an unbuffered La^{3+} solution decreased from pH 7 to pH 5.5–6.0 upon adding 1 mM La^{3+}. At this La^{3+} concentration impurities also sometimes appeared in the solution over time. In addition, recovery of an attractive signal after charge

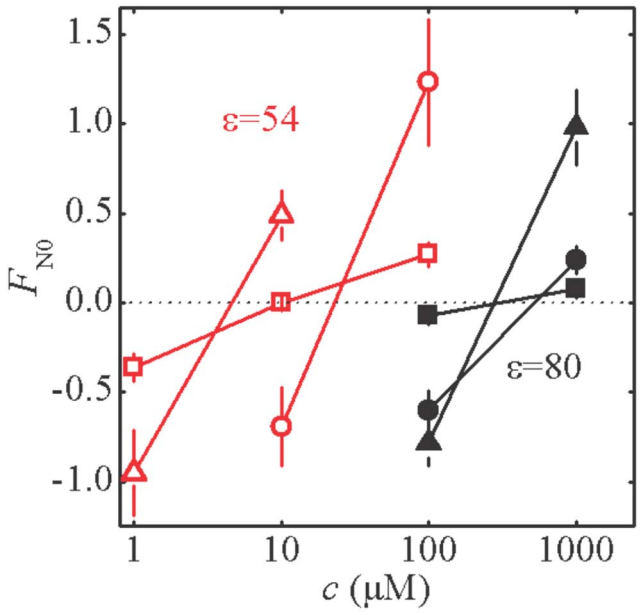

FIG. 5. (Color online) Normalized force F_{N0} versus multivalent ion concentration c for three experiments in which a silica bead was charge inverted using the trivalent ions $[CoC_{12}H_{30}N_8]^{3+}$ (squares), $[Ru(NH_3)_6]^{3+}$ (circles), and La^{3+} (triangles). Electrolytes containing 1 mM HEPES of pH 7.3±0.2 with ϵ=80 (filled symbols) and ϵ =54 (open symbols) were used. The values of c_0 for ϵ=80 and 54 are 300 and 10 μM for $[CoC_{12}H_{30}N_8]^{3+}$, 520 and 23 μM for $[Ru(NH_3)_6]^{3+}$, and 280 and 6 μM for La^{3+}.

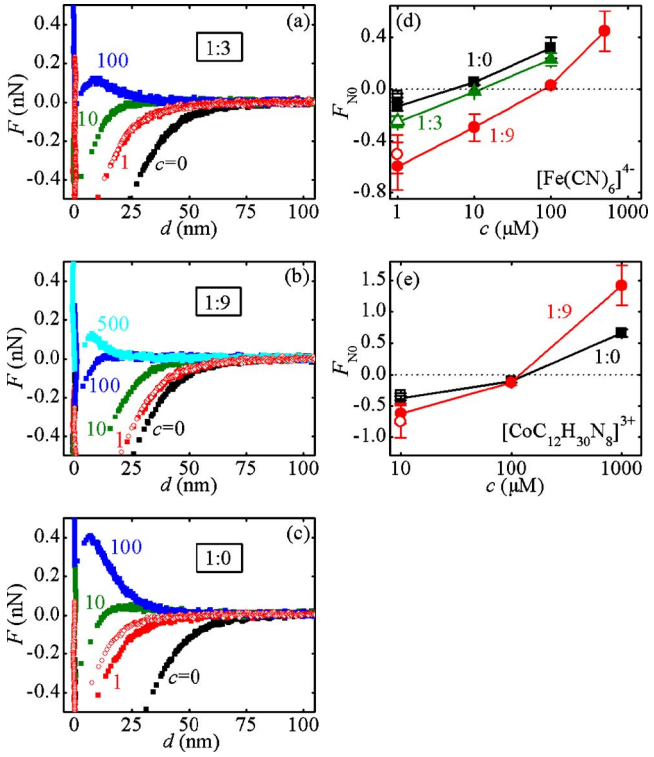

FIG. 6. (Color online) Force versus separation measurements with the same bead and multivalent ion $[Fe(CN)_6]^{4-}$ on three positively charged surfaces prepared with different ratios of 1-trichlorosilyl-11-cyanoundecane:undecyltrichlorosilane, (a) 1:3, (b) 1:9, and (c) 1:0. Solutions also contained 0.5 mM KCl at pH 6.0±0.5. (d) Normalized force F_{N0} versus multivalent ion concentration c for all three measurements. Measurements on the 1:0, 1:3, and 1:9 surfaces are shown as squares, triangles, and circles, respectively. (e) $F_{N0}(c)$ for measurements with a 1:0 and a 1:9 surface using the multivalent ion $[CoC_{12}H_{30}N_8]^{3+}$ in solutions also containing 0.5 mM KCl at pH 7.0±0.5.

inversion had occurred in the ϵ=54 solvent with La^{3+} took three times longer than usual. This indicates a reaction involving La^{3+} in which small quantities of H^+ ions (less than one per 100 La^{3+} ions) are released [3]. This behavior was never observed with ions other than La^{3+}.

VI. SURFACE-CHARGE DENSITY σ_{bare}

We have measured the influence of the bare surface-charge density of the amine-terminated surface on the charge-inversion concentration by changing the amount of chargeable sites on the surface. This was achieved using mixtures of 1-trichlorosilyl-11-cyanoundecane and undecyltrichlorosilane (Gelest) during the preparation of the positively charged surfaces. Undecyltrichlorosilane has a CH_3 end group that is uncharged. Reducing the amount of chargeable groups on the surface correspondingly reduces σ_{bare}. The exact charge ratio on the surface could not be determined reliably because the ratio of charged:uncharged chlorosilanes in the bulk solution cannot be assumed to correspond to the ratio ultimately deposited on the surface. In addition, the preparation of the amine-terminated surfaces is lengthy, and small differences such as the amount of residual water in the solutions and the age of the stock solutions can lead to significant variations in the observed charge-inversion concentration. Here we only compare surfaces with different ratios of charged:uncharged chlorosilane that were prepared simultaneously from the same stock solutions, hence an increase in the charged:uncharged ratio is certain to correspond to an increase in σ_{bare}.

Figures 6(a)–6(d) show an experiment where three positively charged surfaces with different σ_{bare} were charge inverted using the same bead and the quadrivalent ion $[Fe(CN)_6]^{4-}$. Positively charged surfaces were prepared using only 1-trichlorosilyl-11-cyanoundecane (1:0) and ratios of 1-trichlorosilyl-11-cyanoundecane:undecyltrichlorosilane of 1:3 and 1:9. In this particular experiment, measurements were first done with a 1:3 surface [Fig. 6(a)], then with a 1:9 surface [Fig. 6(b)], and finally with a 1:0 surface [Fig. 6(c)]. The order of the measurements rules out that the observed trend is due to aging of the surfaces. Figure 6(d) shows the fitted values of $F_{N0}(c)$ for all three surfaces, showing that decreasing σ_{bare} hinders charge inversion. The values obtained for c_0 are 5, 17, and 74 μM for the 1:0, 1:3, and 1:9 surface, respectively.

Figure 6(e) shows the results of a control experiment where two different, nominally identical silica beads were charge inverted with $[CoC_{12}H_{30}N_8]^{3+}$ and probed using a 1:9 and a 1:0 surface. The measured charge-inversion concentra-

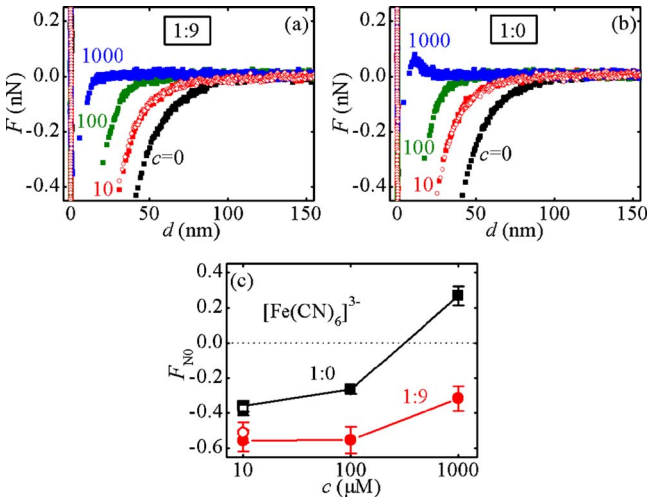

FIG. 7. (Color online) Force versus separation measurements with the same bead and multivalent ion $[Fe(CN)_6]^{3-}$ on two amine-terminated surfaces prepared with different ratios of 1-trichlorosilyl-11-cyanoundecane:undecyltrichlorosilane, (a) 1:9, (b) 1:0. (c) F_{N0} versus c for both measurements. Measurements on the 1:9 and 1:0 surfaces are shown as circles and squares, respectively. Solutions also contained 0.5 mM KCl at pH 6.0±0.5.

tions are 140 and 120 μM using the 1:0 and 1:9 surfaces, respectively. This confirms that the value of σ_{bare} of the positively charged surface has no significant influence on c_0 of a silica bead and that this surface indeed acts as a constant probe.

A similar experiment where 1:9 and 1:0 surfaces were charge inverted using the same bead and the trivalent negative ion $[Fe(CN)_6]^{3-}$ is shown in Fig. 7. The value of c_0 obtained for the 1:0 surface is 320 μM. The 1:9 surface did not exhibit charge inversion at 1 mM $[Fe(CN)_6]^{3-}$. Thus if the 1:9 surface can be charge inverted with $[Fe(CN)_6]^{3-}$ ions, c_0 is higher than 1 mM. Higher concentrations were not probed because λ becomes too short.

VII. DISCUSSION

We first compare our experimental observations with the specific binding description as summarized by Eq. (2). Assuming constant $\Delta\mu^{0*}$, Eq. (2) predicts that $c_0 \sim |\sigma_{bare}/Z|$ and is independent of ϵ. None of these trends agrees with the experiments. We instead observe a decrease of more than an order of magnitude in c_0 when increasing Z from 3 to 4 [2], a decrease in c_0 with increasing σ_{bare} instead of the predicted increase, and a sharp decrease in c_0 with decreasing ϵ.

To reconcile the observations with Eq. (2) it is necessary to let the adsorption energy $\Delta\mu^{0*}$ depend on Z, ϵ, and σ_{bare} and empirically fit its value for each individual measurement. While this approach lacks predictive power, some of the trends observed in the experiment could be rationalized in this way. For example, a more negative $\Delta\mu^{0*}$ might be expected for all ions when the dielectric constant is decreased since this affects ion solubility. The dielectric constant might similarly influence the hydrolysis of metal ions. Two aspects of the data call for a more universal explanation, however.

First, $\Delta\mu^{0*}$ is expected to depend critically on the specific chemical composition of the ions. Although some differences were observed with La^{3+}, the measured c_0 and its dependence on ϵ was similar for three chemically very distinct ions with the same valence.

Second, the observed dependence of c_0 on σ_{bare} implies that binding of the multivalent ions to the surface is coop-

TABLE I. Important parameters for the ion correlation model calculated using Eqs. (3)–(5) and the measured values of c_0 (also shown) for the same ion with different values of ϵ.

Ion	$c_0(\epsilon=80)$ (μM)	$c_0(\epsilon=68)$ (μM)	$c_0(\epsilon=54)$ (μM)	σ_{bare} (e/nm^2)	$\Delta\mu^0$ (units of kT)	$\mu_c(\epsilon=80)$ (units of kT)	$\mu_c(\epsilon=68)$ (units of kT)	$\mu_c(\epsilon=54)$ (units of kT)
$[Fe(CN)_6]^{4-}$	12	5		0.11	−4.1	−4.3	−5.2	
$[Fe(CN)_6]^{4-}$	12		1	0.12	−4.0	−4.4		−6.9
$[Fe(CN)_6]^{4-}$		5	1	0.11	−3.9		−5.4	−7.0
$[Fe(CN)_6]^{3-}$	120		18	0.17	−3.5	−3.3		−5.2
$[CoC_{12}H_{30}N_8]^{3+}$	220	88		−0.28	−2.2	−4.5	−5.4	
$[CoC_{12}H_{30}N_8]^{3+}$	220		14	−0.34	−1.9	−4.9		−7.7
$[CoC_{12}H_{30}N_8]^{3+}$		88	14	−0.37	−1.6		−6.2	−8.0
$[CoC_{12}H_{30}N_8]^{3+}$	300		10	−0.50	−0.8	−6.2		−9.6
$[Ru(NH_3)]^{3+}$	520		23	−0.43	−0.8	−5.6		−8.8
La^{3+}	280		6	−0.63	−0.3	−7.0		−10.9

erative: increasing the density of surface charges facilitates charge inversion. This behavior is not captured by a simple chemical binding picture. This remains true even if a more sophisticated description of the surface is introduced. For example, the surface can be modelled as consisting of discrete sites where multivalent ions compete with other charge-determining ions. Such a model yields an equation similar to Eq. (2) but with a prefactor that is independent of σ_{bare}. That is, it still does not exhibit cooperativity.

We now compare the observations with the ion correlation theory of Eqs. (3)–(5). The latter predicts that $\mu_c \propto -\sqrt{|\sigma_{\text{bare}} Z^3|}/\epsilon$ approximately, and this expression captures very well the direction (increase or decrease) and relative magnitude of the dependence of c_0 on these parameters.

The experimental data permit a more quantitative self-consistency test of this theory. Two unknown parameters enter the model: the surface-charge density at charge inversion, $\sigma_{\text{bare}}(c_0)$, and the residual chemical interaction, $\Delta\mu^0$. Two measurements carried out under slightly different conditions can be used for extracting values for these parameters. We previously showed in this manner that varying Z while keeping the chemical structure constant yields results consistent with $\Delta\mu^0 \approx 0$ [2].

A similar procedure can be used for the measurements at different values of ϵ presented here. Assuming that σ_{bare} and $\Delta\mu^0$ do not depend on ϵ, their values can be deduced from consecutive measurements using the same ion and solvents with different ϵ. The numerical results of this procedure are summarized in Table I, together with the corresponding calculated values of μ_c. In those cases where three values of ϵ were measured, fits were performed pairwise to extract separate estimates of σ_{bare} and $\Delta\mu^0$; the results are consistent within experimental scatter.

We first focus on the results for charge inversion of a silica bead by trivalent positive ions. The fitted values of $\Delta\mu^0$ are in the range $-0.3kT$ to $-2.2kT$. For comparison, the corresponding values of μ_c are in the range $-4.5kT$ to $-10.9kT$. This implies that spatial correlations between multivalent ions are largely sufficient to account for charge inversion. Results for the three different trivalent positive ions are similar, re-iterating that, in spite of anomalies observed with La^{3+}, the chemical composition of these ions does not appear to play a dominant role in determining c_0. Figure 8(a) plots the measured values of c_0 as a function of ϵ for the different experiments, and shows that all of our measurements for silica surfaces are consistent with $\sigma_{\text{bare}} = -0.5\ e/\text{nm}^2$ and $\Delta\mu^0 = -1kT$. Taken together, these observations lend further support to the proposal that a spatial interactions between multivalent ions are the driving mechanism behind charge inversion.

Results for the amine-terminated surfaces are not as clear cut. The calculated values of $\Delta\mu^0$ for charge inversion of the amine-terminated surface by trivalent and quadrivalent negative ions are significantly larger than kT and comparable in magnitude to μ_c. Figure 8(b) shows that the values of c_0 for these measurements can be described by Eq. (3) using $\sigma_{\text{bare}} = 0.14\ e/\text{nm}^2$ and $\Delta\mu^0 = -3.6kT$. In terms of Eq. (3), this suggests that spatial correlations between multivalent ions do not fully account for the observed charge inversion in this case, and that specific binding also plays a role.

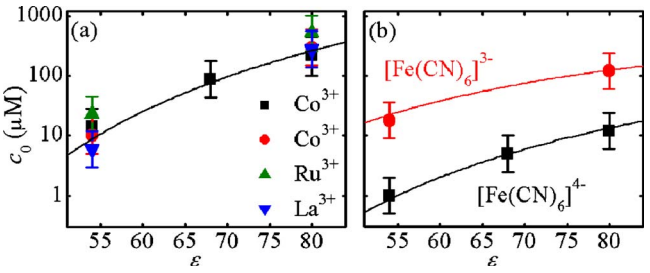

FIG. 8. (Color online) (a) Charge-inversion concentration c_0 versus dielectric constant ϵ for the data shown in Figs. 4(f) and 5. The line is the predicted c_0 versus ϵ according to Eq. (3) with $\sigma_{\text{bare}} = 0.5\ e/\text{nm}^2$, $\Delta\mu^0 = -1kT$, and a typical value $r = 0.4$ nm for the radius of the ions. The error bars represent a factor of 2, which corresponds to the scatter in the data for measurements with the same ion using different, nominally identical beads and amine-terminated surfaces. (b) Same as (a) for the data of Figs. 3 and 4(c). The fitted curves use $\sigma_{\text{bare}} = 0.14\ e/\text{nm}^2$, $\Delta\mu^0 = -3.6kT$, and the real radius of the ions.

One possible reason for this discrepancy is that the calculated values of σ_{bare} of the amine-terminated surfaces correspond to the lower end of the range of validity of the inequality $\Gamma \gg 1$. A similar trend was observed in measurements where Z was varied with low surface-charge densities [2]. Another possible reason is that in the theoretical descriptions discussed here, the charge on the surface is modelled as being continuously distributed whereas real surfaces consist of discrete chemical groups. This disorder can potentially facilitate charge inversion [28,29]. The relative importance of this disorder is expected to increase with decreasing σ_{bare}.

Some caution is necessary in drawing conclusions from the quantitative analysis above, however. If regulation of the surface charge plays a significant role, σ_{bare} depends on the ion concentrations and thus on c_0. The analysis instead assumes that σ_{bare} remains constant. Similarly, both σ_{bare} and $\Delta\mu^0$ can depend on ϵ [30], introducing errors in the quantitative comparison. The degree of consistency between the three calculated values of σ_{bare} and $\Delta\mu^0$ for the measurements with three values of ϵ suggests that treating σ_{bare} and $\Delta\mu^0$ as constants is at least approximately valid, however. To describe the behavior of F_0 away from c_0, regulation of the surface charge has to be considered within the theory. Elucidating the interplay between disorder, regulation and correlations remains an important theoretical challenge.

In summary, we have performed a systematic study of charge inversion by multivalent ions using atomic force spectroscopy. At long range this technique gives a direct, unambiguous measurement of the polarity of the surface being probed. Measurements at shorter range show an additional attractive component of the force, corresponding to constant-potential boundary conditions. We measured the dependence of the charge-inversion concentration on valence, chemical composition, dielectric constant, and surface-charge density, the latter indicating that multivalent ion adsorption is cooperative. These observations are remarkably consistent with a very straightforward description of charge inversion in terms of spatial interactions between multivalent

ions in the Stern layer [16]. To our knowledge, no existing description based on specific adsorption provides a similar degree of agreement, even at a qualitative level. A direct experimental proof of the correlation mechanism, via direct determination of the spatial correlations between multivalent ions at the surface, would be highly desirable.

ACKNOWLEDGMENTS

We thank J. Lyklema, H. A. Heering, and B. Shklovskii for useful discussions and C. Dekker for general support. This work was supported by the "Stichting voor Fundamenteel Onderzoek der Materie" (FOM) and the "Netherlands Organization for Scientific Research" (NWO).

[1] V. A. Bloomfield, Biopolymers **44**, 269 (1997).
[2] K. Besteman *et al.*, Phys. Rev. Lett. **93**, 170802 (2004).
[3] R. O. James and T. W. Healey, J. Colloid Interface Sci. **40**, 42 (1972); **40**, 53 (1972); **40**, 65 (1972).
[4] A. Martín-Molina *et al.*, J. Chem. Phys. **118**, 4183 (2003).
[5] R. Messina, C. Holm, and K. Kremer, Phys. Rev. Lett. **85**, 872 (2000).
[6] M. Tanaka and A. Y. Grosberg, Eur. Phys. J. E **7**, 371 (2002).
[7] R. M. Pashley, J. Colloid Interface Sci. **102**, 23 (1984).
[8] K. B. Agashe and J. R. Regalbuto, J. Colloid Interface Sci. **185**, 174 (1996).
[9] V. Vithayaveroj, S. Yiacoumi, and C. Tsouris, J. Dispersion Sci. Technol. **24**, 517 (2003).
[10] For comprehensive reviews, see A. Yu. Grosberg, T. T. Nguyen, and B. I. Shklovskii, Rev. Mod. Phys. **74**, 329 (2002);Y. Levin, Rep. Prog. Phys. **65**, 1577 (2002);M. Quesada-Pérez *et al.*, ChemPhysChem **4**, 234 (2003).
[11] E. S. Reiner and C. J. Radke, Adv. Colloid Interface Sci. **47**, 59 (1993).
[12] S. H. Behrens and D. G. Grier, J. Chem. Phys. **115**, 6716 (2001).
[13] J. Lyklema and J. F. L. Duval, Adv. Colloid Interface Sci. **114**, 27 (2005).
[14] R. Zhang and B. I. Shklovskii, Phys. Rev. E **72**, 021405 (2005).
[15] R. Pericet-Camara *et al.*, J. Phys. Chem. B **108**, 19467 (2004).
[16] B. I. Shklovskii, Phys. Rev. E **60**, 5802 (1999).
[17] H. Totsuji, Phys. Rev. A **17**, 399 (1977).
[18] I. Rouzina and V. A. Bloomfield, J. Phys. Chem. **100**, 9977 (1996).
[19] J. Ennis, S. Marcelja, and R. Kjellander, Electrochim. Acta **41**, 2115 (1996).
[20] W. A. Ducker, T. J. Senden, and R. M. Pashley, Langmuir **8**, 1831 (1992).
[21] Sum of metal ion radius and ligand (H_2O, NH_3, CN^-) diameter. The radii are comparable (within 4%) to crystallographic data.
[22] R. D. Shannon, Acta Crystallogr., Sect. A: Cryst. Phys., Diffr., Theor. Gen. Crystallogr. **A32**, 751 (1976).
[23] Y. Marcus, *Ion Properties* (Marcel Dekker Inc., New York, 1997), Chap. 3.
[24] Measurements were done at *p*H less than the first hydrolysis constant of La^{3+}; J. Burgess, *Metal Ions in Solution* (Ellis Horwood, Chichester, England, 1979), Chap. 9.
[25] From crystal structure with van der Waals radii; A. Bacchi, F. Ferranti, and G. Pelizzi, Acta Crystallogr., Sect. C: Cryst. Struct. Commun. **C49**, 1163 (1993).
[26] G. Telléz and E. Trizac, Phys. Rev. E **70**, 011404 (2004).
[27] G. Arscott and V. A. Bloomfield, Biopolymers **36**, 345 (1995).
[28] A. G. Moreira and R. R. Netz, Europhys. Lett. **57**, 911 (2002).
[29] M. L. Henle *et al.*, Europhys. Lett. **66**, 284 (2004).
[30] F. A. Rodrigues, P. J. M. Monteiro, and G. Sposito, J. Colloid Interface Sci. **211**, 408 (1999).